System concept for a moderate cost Large Deployable Reflector (LDR)

Paul N. Swanson
James B. Breckinridge, MEMBER SPIE
Alan Diner
Robert E. Freeland
William R. Irace
Paul M. McElroy
Aden B. Meinel, MEMBER SPIE
A. Fernando Tolivar
Jet Propulsion Laboratory
California Institute of Technology
4800 Oak Grove Drive
Pasadena, California 91109

Abstract. A study was carried out at the Jet Propulsion Laboratory during the first quarter of 1985 to develop a system concept for NASA's Large Deployable Reflector (LDR). This new system concept meets the primary scientific requirements and minimizes the cost and development time. The LDR requirements were investigated to determine whether or not the major cost drivers could be significantly relaxed without compromising the scientific utility of LDR. In particular, the telescope wavefront error is defined so as to maximize scientific return per dollar. Major features of the concept are a four-mirror, two-stage optical system; a lightweight structural composite segmented primary reflector; and a deployable truss backup structure with integral thermal shield. The two-stage optics uses active figure control at the quaternary reflector located at the primary reflector exit pupil, allowing the large primary to be passive. The lightweight composite reflector panels limit the short wavelength operation to approximately 30 μm but reduce the total primary reflector weight by a factor of 3 to 4 over competing technologies. System optical performance is calculated including aperture efficiency, Strehl ratio, and off-axis performance. On-orbit thermal analysis indicates a primary reflector equilibrium temperature of less than 200 K with a maximum gradient of $\approx$5° C across the 20 m aperture. Weight and volume estimates are consistent with a single Shuttle launch and are based on Space Station assembly and checkout.

Subject terms: large optics technology; Large Deployable Reflector; infrared astronomy; submillimeter astronomy; two-stage optics.

Optical Engineering 25(9), 1045-1054 (September 1986).

CONTENTS

Invited Paper LO-105 received Feb. 15, 1986; revised manuscript received March 31, 1986; accepted for publication May 26, 1986; received by Managing Editor June 10, 1986. This paper is a revision of Paper 571-44 which was presented at the SPIE conference on Large Optics Technology, Aug. 19-21, 1985, San Diego, Calif. The paper presented there appears (unrefereed) in SPIE Proceedings Vol. 571.

1. INTRODUCTION

The Large Deployable Reflector (LDR) is a dedicated astronomical observatory to be placed in orbit above the earth's obscuring atmosphere. It will operate in the spectral range between 30 and 1000 μm wavelength. The observatory was recommended by the National Academy of Sciences Astronomy Survey Committee[1] (Field Committee) as one of the four major astrophysical projects of the 1980s. The NASA Office of Space Science and Applications (OSSA) has scheduled the LDR for a new start sometime in the 1990s, immediately after the Shuttle Infrared Telescope Facility (SIRTF) and the Advanced X-Ray Astrophysics Facility (AXAF). Recent reviews of the LDR are given in the references.[2-6]

Two workshops have been held to broaden participation in the LDR, to solidify the concept, and to define the LDR technology development requirements. The first LDR Asilomar workshop[7] was held in Pacific Grove, Calif., in June 1982. The second LDR Asilomar workshop was held in March 1985. The results of the present study were presented at the March 1985 workshop.

2. STUDY OBJECTIVES AND APPROACH

Concepts for LDR have been studied by many groups since 1978. Recently LDR concepts have become more complex and have increased noticeably in both cost and weight. A subgroup of NASA's LDR Science Coordination Group,

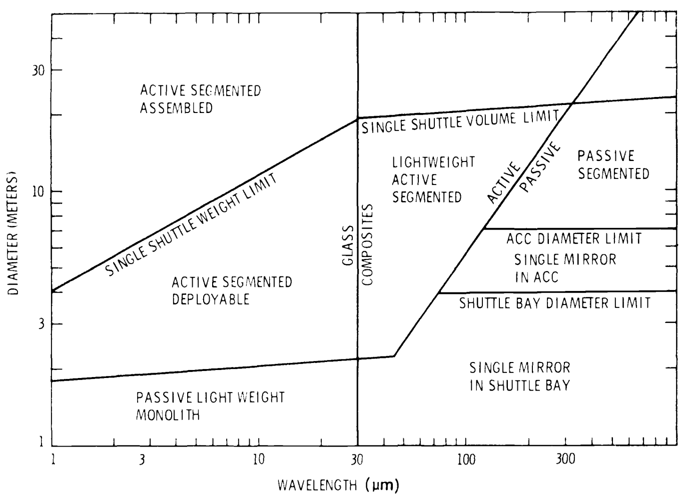

Fig. 1. Wavelength-diameter plane for LDR showing major technology breaks and regions of particular configurations.

concerned about cost and scope growth in recently developed LDR concepts, met at the University of Arizona in November 1984. The purpose of the meeting was to consider whether an LDR could be approached as a scaled-up radio telescope rather than a scaled-down optical telescope. In response to this meeting and to the authors' similar concerns about the future of the LDR, the Jet Propulsion Laboratory (JPL) commissioned the present study to define a "minimum" LDR that met the science requirements while keeping the cost and complexity at a minimum. The study approach was to start with millimeter wavelength radio telescope technology and see how far it could be pushed in the direction of shorter wavelengths and larger diameters. The assumption was that if the LDR science requirements could be met, this would result in the lightest and least expensive system configuration.

Figure 1 shows the wavelength-diameter plane relevant to LDR and indicates major technology breaks. The 20-m-diameter, 30-μm-wavelength LDR is near the intersection of several limits in the upper center of the figure. The least difficult approach is based on lightweight composite, actively controlled, segmented telescope technology represented by the right central region of the figure.

The recent development of lightweight graphite epoxy-honeycomb primary reflector panels of high precision and the concept of two-stage optics gave encouragement that the LDR requirements could be met.

3. LDR CONCEPT SUMMARY

The present JPL concept for the LDR telescope as shown in Fig. 2 is based on a 20-m-diameter reflector. The primary mirror is a filled aperture made up of 84 hexagonal panels, each approximately 2 m edge-to-edge. The panels are based on lightweight structural composite materials. The optical configuration is a four-mirror, two-stage system (described in Sec. 7). The primary mirror is passive. The active optical elements for figure control are at the quaternary mirror. The primary mirror panels are supported by a deployable "PAC truss"* backup structure at the vertices of each hexagon.

*PAC truss, a term coined by John Hedgepeth, is derived from the popular video game PAC MAN. It refers to a specific structure developed by Hedgepeth and the NASA Langley Research Center.

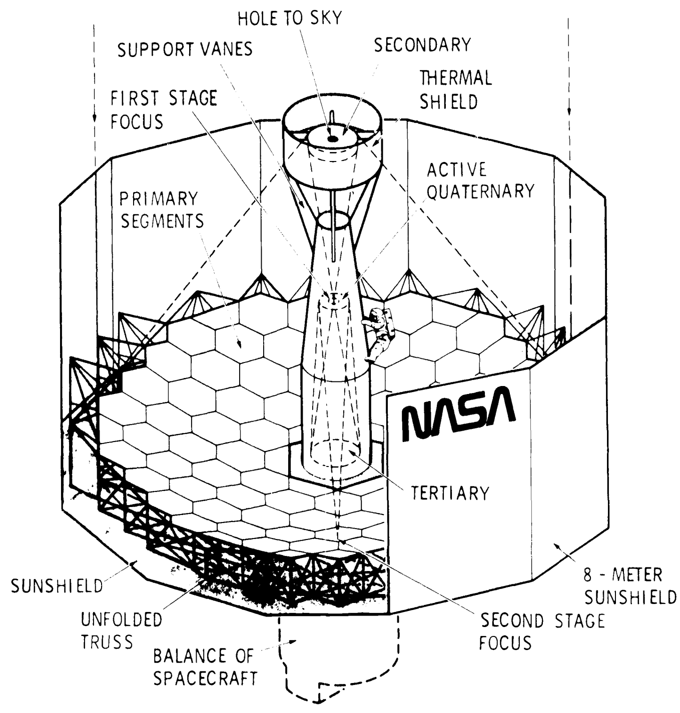

Fig. 2. LDR telescope configuration.

The four focal plane instruments covering the range of 30 to 1000 μm are located near the vertex of the primary mirror. Some of the instruments will be cooled with stored cryogens to liquid helium temperatures, others to liquid nitrogen temperatures.

The spacecraft functions such as power, communications, data system, attitude control, etc., will be located in a resource module behind the primary mirror.

The LDR will be transferred to orbit by the Space Transportation System (STS) and assembled and tested at the Space Station. It will then be boosted to an orbit of $\gtrsim$700 km as a free flyer.

4. SYSTEM REQUIREMENTS

The system requirements have evolved over the years and are summarized by Swanson et al.[2]; the current versions are listed in a JPL internal report.[8] It was determined in the study that several of these requirements were strong system drivers and that a relaxation or a better definition of some of the requirements could reduce system complexity, weight, and cost by a large amount.

The requirements that were identified as system drivers were the "light-bucket" operation at 1 to 4 μm, the primary optics temperature uniformity of 1 K, and a sun exclusion angle of 60°. The light-bucket mode of operation drives the surface figure to nearly optical tolerances and thus was given up entirely. The primary mirror uniformity of 1 K was driven by the need to spatially chop the beam by rocking the secondary mirror, thereby introducing an intensity modulation of the signal if large temperature gradients existed across the primary. It was determined that spatial chopping could be accomplished at the quaternary mirror of the two-stage optical system, eliminating the 1 K uniformity requirement. Increasing the sun exclusion angle to 90° from 60° greatly simplified the primary reflector sunshade design.

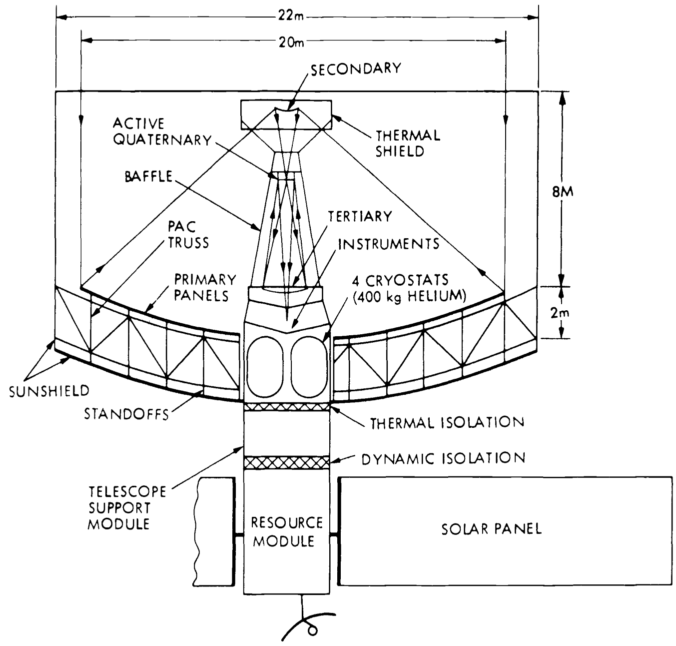

Fig. 3. LDR system configuration, side view.

5. SYSTEM FUNCTIONAL ARCHITECTURE

The objective of the system functional architecture is to allocate functions among distinct subsystems in order to provide for a logical grouping of compatible functions, to simplify interfaces among subsystems, to facilitate system design, procurement, test, assembly, and operations, and to provide an efficient means of meeting functional requirements.

Four subsystems meeting these objectives are identified: an optical system, an instrument module, a telescope support module, and a resource module. These can be seen in the LDR side view in Fig. 3. Each of the four may be envisioned to be sufficiently independent from the other three so that it may be designed and fabricated by a separate organization under the direction of a single system integrator (a mode of development that is likely for a facility as large as LDR). A brief description of the functions of each subsystem follows.

5.1. Optical system

The optical system consists of reflector optical surfaces, their support structures, the structural reference frame for the instrument module, sunshade, adaptive optics sensors and controllers, and fine pointing sensors and controllers.

5.2. Instrument module

The instrument module consists of the science instrument assemblies, their associated cooling apparatus (which could be integrated into each instrument or serve several instruments), cold instrument electronics (optics and front-end electronics), fine and coarse attitude sensors (which require access to the focal plane), and "pick-off" optics to route the telescope images to various instruments in the module.

5.3. Telescope support module

The telescope support module is the buffer between the predominantly science-oriented equipment and the predominantly engineering-oriented equipment of the LDR. It consists of all the housekeeping equipment that is directly required by the instrument module and optical system, as well as all the equipment required to make the optical system, instrument module, and telescope support module compatible with a pre-existing carrier platform (called the resource module).

TABLE I. System weight and power summary.

System	Weight (kg)	Power (kW)
Optical system	6,876	0.42
Instrument module	3,372	0.15
Telescope support module	1,237	2.7
Resource module	6,133	3.8
Consumables	2,629	0
Total	20,274	7.1

5.4. Resource module

The resource module is envisioned as the carrier platform for the LDR. It provides typical spacecraft functions such as power generation and preconditioning, power storage, telecommunications, course attitude control, central computing and data handling, propulsion for orbit sustenance, and possibly orbit raising/lowering. System weight and power are summarized in Table I.

6. MINIMUM OPERATING WAVELENGTH, SURFACE ERROR, AND TELESCOPE PERFORMANCE

The concept of antenna gain is widely used for radio telescopes and is useful in defining the relationship between optical surface error and minimum operating wavelength for LDR. The gain is given by the equation

$$G = \left(\frac{\pi D}{\lambda}\right)^2 \eta \exp\left[-\left(\frac{4\pi\sigma}{\lambda}\right)^2\right] , \qquad (1)$$

where

σ = rms surface error ,

D = aperture diameter ,

η = geometric efficiency ,

$\exp\left[-\left(\frac{4\pi\sigma}{\lambda}\right)^2\right]$ = Strehl ratio .

The rms surface error σ has a spatial correlation length associated with it. A correlation length term can be included in Eq. (1). However, its effect is to increase the gain in Eq. (1) by a negligible amount for short correlation lengths (<50 cm for LDR). For very long correlation lengths, the gain may increase by a factor of 2. The geometric efficiency η is determined by aperture and illumination taper. It is usually $\simeq 0.6$ for high gain radio telescopes with large edge taper and approaches unity for unblocked, uniformly illuminated optical telescopes. It can be shown that the gain peaks at a value of $\sigma/\lambda = 1/4\pi$. This value of $\lambda/\sigma = 4\pi$ is often used as the criterion for minimum operating wavelength. As a further refinement, it has been shown by Von Hoerner[9] that the cost of a large radio telescope varies according to

$$\text{cost} = K \frac{D^n}{\sigma^m} , \qquad (2)$$

where

D = diameter ,

n ≈ 2.5 , $(2 < n < 3)$,

m ≈ 1.5 , $(1 < m < 3)$,

K = constant .

Therefore, the ratio of gain/cost, rather than just the gain, can be maximized. The gain/cost function is similar to the gain function except that the former peaks at $\lambda/\sigma = 4\pi\sqrt{n/m} = 16.2$. Thus, for a given minimum operating wavelength, a telescope will have a maximized gain/cost when the rms surface errors are $\lambda_{min}/16$. For LDR at 30 μm, the rms surface error should be $\lesssim 2$ μm. Of course, improving the surface error improves the telescope performance at 30 μm but increases the cost. It results in a telescope optimized at a shorter wavelength than the desired 30 μm.

Equation (2) is based on experience with large ground-based radio telescopes. Since LDR is structurally similar to ground-based radio telescopes, the form of the scaling law should be the same. However, the values for m and n may differ somewhat for a space-based telescope with a very large D/λ.

General performance predictions can be made for a large aperture reflecting telescope that are, in general, independent of the specific design.

In Eq. (1), the last two terms are called the aperture efficiency; that is,

$$\text{aperture efficiency} = \eta \text{ Strehl} . \quad (3)$$

For the criterion of $\lambda_{min}/\sigma = 16$ and a geometric efficiency of $\eta > 0.6$, we get

$$\text{aperture efficiency} > 0.6 \exp\left[-\left(\frac{4\pi}{16}\right)^2\right] = 0.32 . \quad (4)$$

This exceeds the LDR requirement of 0.3 given in Ref. 8.

Far-field radiation patterns, or alternatively Airy patterns in the focal plane, may be calculated by knowing the primary reflector diameter, primary illumination, wavelength, rms surface error, and its spatial distribution. The patterns shown in Fig. 4 are calculated after an analysis by Vu.[10] Five curves are shown for rms surface errors from 0 to 4 μm. The nominal 2 μm surface error is the middle curve. G/G(0) is the normalized on-axis gain and shows the effect of increasing surface error. The beam percentage is the integrated power out to the first null (sometimes called the central fringe), and theta-3 dB is the full beamwidth at half power.

The normalized power patterns can be integrated out to a 1 arcsec radius (2-arcsec-diameter circle) for various wavelengths, surface errors, and correlation lengths. Integrations were performed for $\sigma = 2$ μm, correlation lengths from 1 m to 25 cm, and wavelengths from 1 to 100 μm. At the nominal 30 μm wavelength, more than 50% of the energy will fall on a 2 arcsec detector for correlation lengths of >25 cm. However, in the light-bucket mode, below 10 μm, only 15% of the energy will fall on a 2 arcsec detector if the correlation length is greater than 1 m. If the correlation length is less than 25 cm, virtually none of the radiation will fall on the detector. Therefore, for a 2 μm surface error, operation below 10 to 20 μm in the light-bucket mode is doubtful.

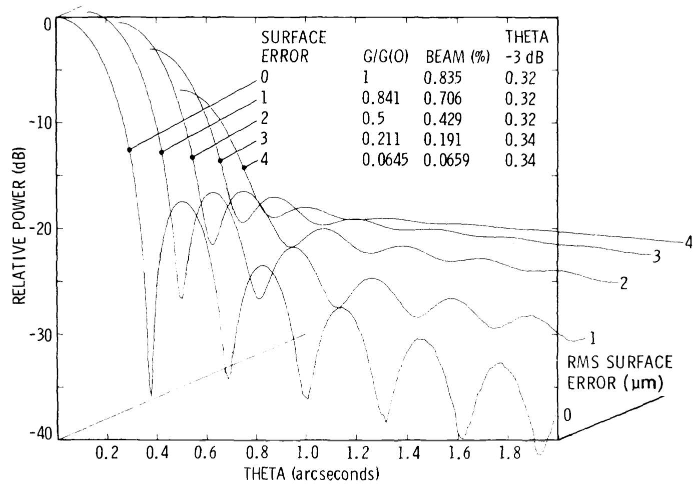

Fig. 4. Power patterns for a 20 m LDR operating at a wavelength of 30 μm, uniformly illuminated aperture with rms surface errors of 0, 1, 2, 3, and 4 μm. Surface error correlation length is 1 m.

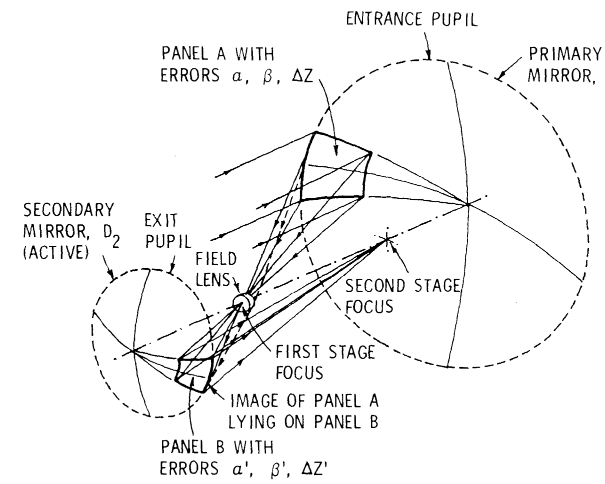

Fig. 5. A Gregorian configuration clearly illustrates the optical principles of a two-stage system, using, in this case, a field lens to reimage the primary onto the active secondary. The simplest configuration embodying this concept is a Gregorian plus a field lens. $\alpha' = \alpha M$, $\beta' = \beta M$, $\Delta z' = \Delta z$, $M = D_2/D_1$ = magnification.

7. OPTICAL SYSTEM DESCRIPTION

The key to the optical approach is to upgrade the performance through a two-stage optics concept.[11] In this concept, the first stage is a segmented 20-m-diameter mirror that forms an approximate image. The second stage "tunes up" the wavefront to the desired high acuity. The optical element that does this tuning is a small monolithic structure located at a real image of the primary mirror. These miniature mirror segments are arranged in an identical pattern to the primary mirror segments and are actively adjusted so that each segment causes the reflected wavefront to be perfectly phased and directed to a common focus in the LDR experiment package.

The general optical principle of a two-stage system is shown in Fig. 5. In this system, the image of the primary is formed by a small field lens placed at the focus of the primary mirror. The concave Gregorian secondary is placed at this image of the primary, relaying the object field to the second stage focus on the optical axis ahead of the primary mirror. An individual primary mirror panel has tip, tilt, and piston errors. A corresponding mirror panel of the secondary lies

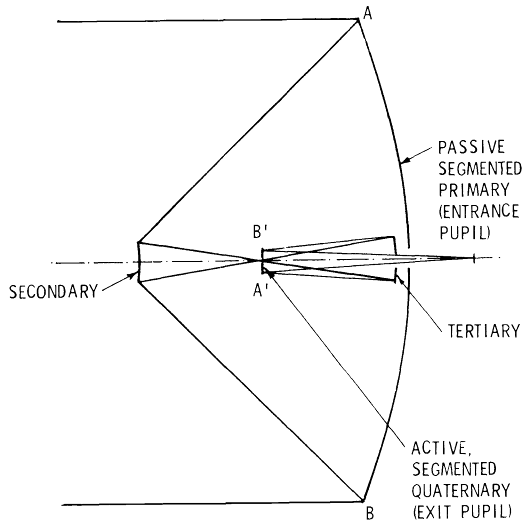

Fig. 6. A four-mirror two-stage configuration applicable to LDR. The tertiary mirror acts like the field lens of Fig. 5, forming the image of the primary on a flat, active quaternary mirror. This geometry was used to obtain the computer simulation results.

coincident with the image of the primary panel. The approximate tip, tilt, and piston corrections to be applied to the secondary panel are related to the magnification of the primary and secondary (as shown in Fig. 5). Exact relationships are utilized in the computer modeling work reported in Sec. 8.

The key role of the field lens is this: if the ray bundle from the primary is directed toward the field lens, but at a small angle off from the rays (shown in Fig. 5), the field lens bends them back so that they arrive at the secondary at the exact places where the rays originated from the primary. The maximum tip and tilt error that the system can correct is therefore set by the aperture diameter of the field lens.

The four-mirror configuration for the LDR two-stage optics, shown in Fig. 6, is optically identical to that in Fig. 5, but in this case the tertiary serves as the field element, forming the image of the primary on the active, segmented quaternary. Note that points A and B in the entrance pupil (the primary) are imaged at points A′ and B′ at the exit pupil (the quaternary). The two-stage optics concept leads directly to a number of advantages:

(1) Initial figure errors in the individual primary reflector segments for correlation lengths greater than a few centimeters may be completely compensated for by forming the conjugate figure in the corresponding quaternary segments. Therefore, the primary mirror may utilize the lower optical quality, lightweight composite panel technology to bring the LDR system weight to within a single-Shuttle launch capability.

(2) Wavefront control at the quaternary reflector is done by a small sophisticated integral unit, which consists of small actuators supported by a stiff substrate; thus, this unit eliminates the need to have on-orbit assembly of a complex array of actuators, sensors, and electrical interconnections associated with an active primary reflector. The result is a small unit that can be completely assembled and tested prior to launch and carried fully assembled in the Space Transportation System (STS).

(3) The field-chopped beam is stationary on the primary; hence, the signal as seen by the detectors is independent of a temperature gradient on the primary mirror. The beam motion on the secondary and tertiary mirrors is small.

8. OPTICAL ANALYSIS AND MODELING

A computer simulation of the two-stage concept shows that it is a feasible approach for correcting large, fast, long-wavelength telescopes. With the optical design code ACCOS V, simple segment tilt and piston errors are simulated as spline deformations on top of the initial figure. The segment tilt and piston errors are added to the primary reflector deformations. These errors are reimaged to a pupil and corrected with simple tilt and piston deformations simulated with spline surfaces on the quaternary. The resultant imagery of the corrected system, measured by the Strehl ratio, maintains a high Strehl ratio, even with relatively large deformations.

The deformations added to the primary surface are position errors of the 0.6 to 0.8 fractional annulus along the optical axis and tilt errors of the same annulus about the 0.7 point. The deformation magnitudes are +1, +2, and +4 mm for the piston of the primary annulus and 0.1, 0.2, and 0.5 mrad for the tilt of the primary annulus. Similar monolithic changes are made to the corresponding annulus on the quaternary with some tilt corrections to account for changes in focal length. Larger tilt magnitudes of 1 and 2 mrad are considered for a quaternary with additional refocusing (a curvature change).

Results for the Strehl ratio at a wavelength of 30 μm versus half field angle are shown in Figs. 7 and 8 for piston and tilt error, respectively. Figure 9 is for a segment tilt error of 1 and 2 mrad with tilt and refocus of the quaternary. For the required 3 arcmin field of view, the Strehl ratio drops less than 3% for corrected piston error of 1 mm, less than 5% for corrected tilt error of 0.1 mrad, and less than 5% for tilt error of 1 mrad corrected with refocus. A tilt error of 1 mrad corresponds to a sag at the edge of the annulus of 1 mm. A linear combination of 0.1 mrad tilt with a 2 mm piston error will be a surface slope from 1.9 to 2.1 mm and will be correctable with a resultant Strehl ratio greater than 0.9. The usable half field angle in each case is 2 arcmin. A brief sensitivity analysis shows that no major optical problems arise from the two-stage correction.

The analysis shows the most severe problems to be with the secondary because of its high magnification. For a corrected 2 mm piston error, the initial Strehl ratio on-axis is 0.96. The Strehl ratio degrades to approximately 0.8 to 0.9 for decenter, tilt, and piston errors of 0.4 mm, 300 μrad, and 5 mm, respectively. These are relatively large errors on this element. Errors on other elements will have less effect.

Field chopping by tilting the Cassegrain secondary about its vertex is a standard and an essential aspect of infrared astronomical observations. The large size of the LDR and the relatively fast focal ratio of 10 mean that the secondary is larger than 1 m in diameter. Chopping this large mirror at several hertz produces a large periodic disturbance to the LDR structure, and, even with momentum compensation, it could be a serious disturbance to accurate pointing.

A serious astronomical problem resulting from vertex chopping is the image degradation resulting from the LDR length limitation that requires the primary focal ratio to be on the order of f/0.6. The resultant coma causes the Strehl ratio to reach zero at a chop angle of only 30 arcsec. The alternative mode is to pivot the secondary about its neutral point, which results in zero coma. The problem with this solution is that the

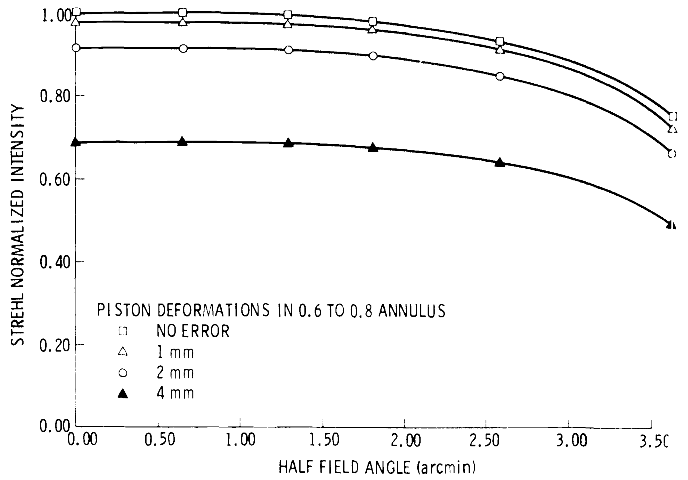

Fig. 7. Variation of the Strehl ratio vs half field angle at 30 μm for given piston errors on the primary.

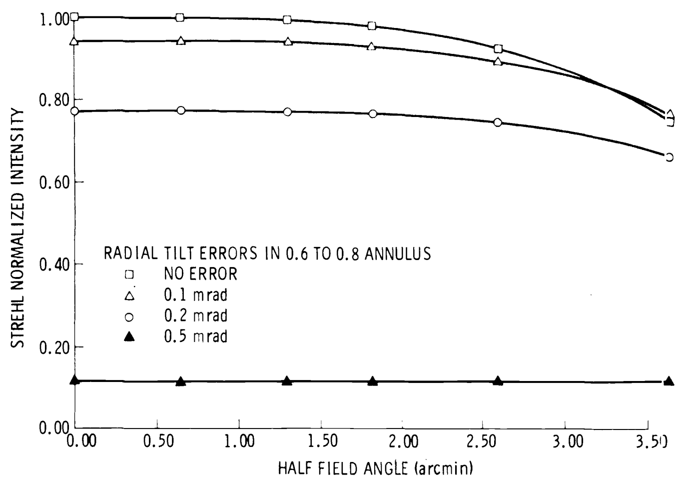

Fig. 8. Variation of the Strehl ratio vs half field angle at 30 μm for given tilt errors on the primary.

secondary mirror translates laterally in the field of view of the detector, thus introducing a potentially serious modulation of the infrared signal.

The present option for chopping is by means of tilting the quaternary mirror about its vertex. The quaternary is half the diameter of the Cassegrain secondary, reducing the momentum problem. The quaternary also is flat, thus producing no image degradation over the chop angle, thereby maintaining a constant Strehl ratio. Lastly, tilting the quaternary is the only chopping option that holds the beam stationary on the primary mirror.

9. PRIMARY REFLECTOR SUPPORT STRUCTURE DESCRIPTION

The primary reflector truss structure provides support for the segmented primary reflector and for the reflector 10 m sunshield and its support structure. It attaches to the optical bench, which will be preassembled and aligned before launch. The optical bench is the primary load-carrying structure for the LDR during boost. The primary reflector support structure is a self-deployable PAC truss that passively supports 84 2-m-diameter structural composite panels. The sunshield support structure, which consists of thin wall composite

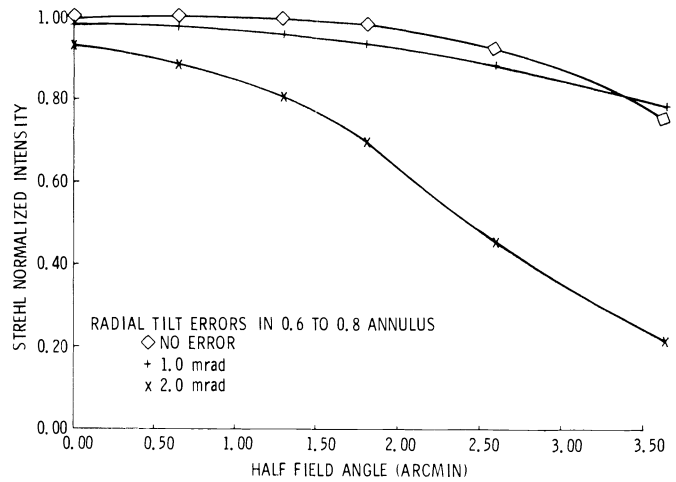

Fig. 9. Variation of Strehl ratio vs half field angle at 30 μm for given tilt errors on the primary with refocus of the system to optimize the image.

tubes, terminates at the perimeter of the truss and deploys as an integral part of the PAC truss. The sunshield itself consists of multilayer insulation (MLI) blankets that either deploy from canisters attached from its support structure or unfold as part of the truss deployment sequence. The deployed truss structure, with Space Station assembly capability, will be mounted to the optical bench. The primary reflector panels will be mounted on the truss structure, checked for alignment relative to a best fit parabola, and then adjusted by means of their interface hardware with the truss.

The PAC truss is based on a unique self-deployable truss concept that was conceived at the Langley Research Center and developed by the Astro Aerospace Corp. The PAC truss concept, in particular, has the advantage that the deployment is inherently strongly synchronized. This synchronized deployment is accommodated by a large number of single-degree-of-freedom hinge-type joints. The excellent mechanical packaging efficiency results from a double-fold scheme where the stowed width of one bay is equal to 3.5 tube diameters and the stowed package height is equal to twice the depth of the deployed truss. The triangular shape of the cells of the truss lends itself nicely to three support points (nodes) for each reflector panel. Since the vertical truss members remain parallel during all phases of deployment, the support posts for the sunshield can be integrated at the perimeter of the truss and not interfere with its deployment. This concept truss, like other generic truss structures, has good deployed stiffness.

A one-quarter scale, kinematic proof-of-concept model of the LDR primary reflector PAC truss has been developed and is shown in Fig. 10. The purpose of the three-dimensional, six-cell model is to demonstrate the deployment scheme, the synchronization associated with deployment, and the mechanical packaging efficiencies of the concept.

10. SUPPORT STRUCTURE MECHANICAL PERFORMANCE

The tolerance for the panel support points on the truss after deployment and adjustment is estimated to be ≤100 μm rms from a best fit theoretical surface. The total mass of the truss structure is 1600 kg, which amounts to an areal density of approximately 5 kg/m^2. The mass of the 10-m-long sunshield, support posts, the 20-layer MLI sunshield, and the 77-layer

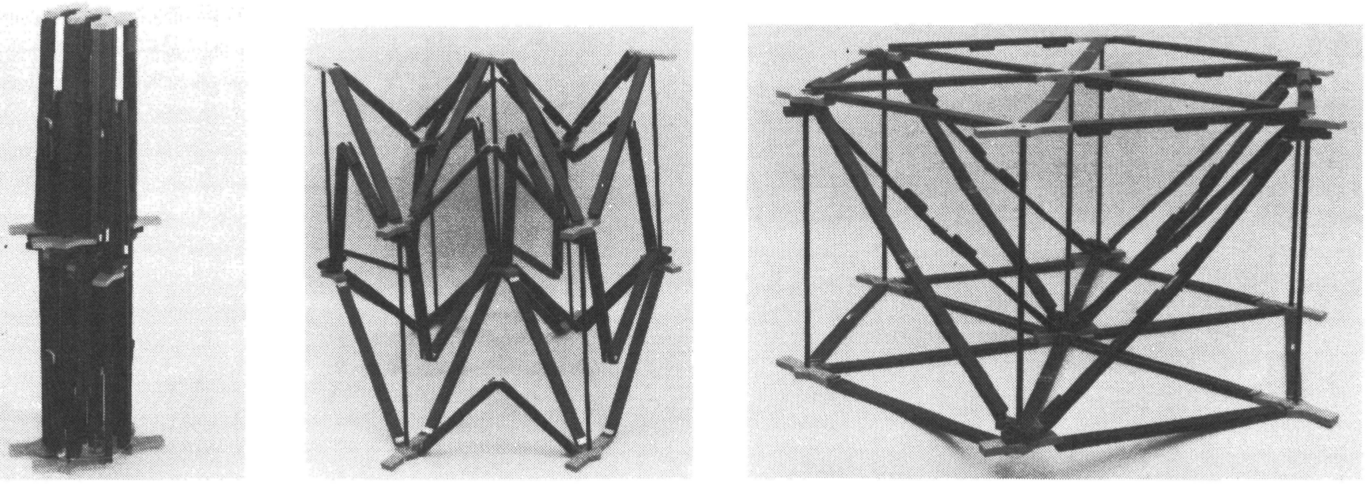

(a) (b) (c)

Fig. 10. Single bay, 1/4 scale, kinematic proof-of-concept model of the LDR primary reflector PAC truss. (a) Stowed; (b) partially deployed; (c) fully deployed.

MLI bottom sunshield is 700 kg. The stowed truss volume is 1×1×4 m. However, when the 10-m-long sunshield support tubes are integrated with the truss, the length of the stowed volume increases to 10 m. The elastic deformation of the truss during slew is estimated to be ≈2.5 μm rms from its reference position for a reflector panel mass of 10 kg/m^2. The thermal distortion of the panel support points for a temperature gradient of 10 K across the truss is estimated to be 40 μm rms. The lowest natural frequency of the truss structure is >1 Hz for panels with a mass of 10 kg/m^2.

TABLE II. Measured mirror figure change with temperature for a 60 cm CFRP sandwich panel made by Dornier.

Temperature (°C)	20.0	−7.5	−34.5	−56.2
Focus (μm)	−0.4±0.5	3.0±0.5	2.9±0.9	7.8±1.8
Astigmatism (μm)	0.9±0.6	1.7±1.2	2.8±1.8	3.1±2.8
Astigmatism angle (degrees)	19	−58	−60	4
rms figure change including astigmatism and focus (μm)	0.3	1.0	1.2	2.5
rms figure change with astigmatism and focus removed (μm)	0.2	0.4	0.6	0.8

11. REFLECTOR PANELS

The primary reflector is a driver in the overall LDR design. Its mass, surface figure, and thermal behavior affect most of the other LDR subsystems. It has to be lightweight, low cost, thermally stable, and structurally stiff to accommodate the given requirements. Because of these requirements, composite sandwich panels turn out to be one of the most attractive candidate materials for use as the primary reflector for the LDR. These panels must have high initial precision and must maintain on-orbit surface stability to within approximately 2 μm rms. Long-term dimensional stability, which includes moisture effects, microcracking, ultraviolet (UV) degradation, and atomic oxygen erosion, must be addressed.

The composite panels evaluated by JPL were developed by Dornier Systems, Friedrichshafen, Federal Republic of Germany, and Hexcel Corporation, Dublin, Calif. All of the prototype panels were a sandwich construction using carbon-fiber reinforced plastic epoxy (CFRP) facesheets bonded to aluminum honeycomb cores. Facesheet materials investigated included graphite/epoxy (Gr/Ep), Kevlar/Ep, glass/Ep, SiC/Ep, and their hybrids. Dornier Systems provided JPL with the largest panels (60 cm square). These panels were homogeneous designs using Gr/Ep facesheets and an aluminum core. Hexcel Corporation provided smaller panels (≈25 cm square) using a variety of panel material constructions.

The composite reflector panels were tested in a thermal chamber at the University of Arizona by using a 10.6 μm laser interferometer to evaluate overall surface figure changes as a function of temperature. These data were obtained manually and digitally and then analyzed using the University of Arizona optical fringe program. The mirror figure changes for both the Dornier and Hexcel panels showed that these panels were thermally stable on the order of a few micrometers at near-orbital temperatures with little thermal hysteresis. Focus and astigmatism were the main optical parameters found to be affected by the test. Table II shows typical test results for a 60 cm panel produced by Dornier.

The lowest test temperature is approximately 15° C higher than the LDR reflector temperatures expected in orbit; therefore, the thermal distortion measured is representative of an actual LDR panel of comparable size. Larger panels that will be used in LDR will have proportionally larger thermal distortions. However, if the initial orbital surface figure can be predicted before launch, the major errors of focus and astigmatism may be compensated for by manufacturing the complementary error in the much smaller quaternary segments, which map one-for-one from the primary to the quaternary. Therefore, the appropriate errors to be considered are the uncompensated errors in the last row of Table II.

At this time the Hexcel panels have not been completely analyzed. However, preliminary results on the 25 cm panels show an initial rms surface error of less than a micrometer with high specularity after aluminum coating. The thermal behavior appears to be equal to or better than that of the Dornier panels.

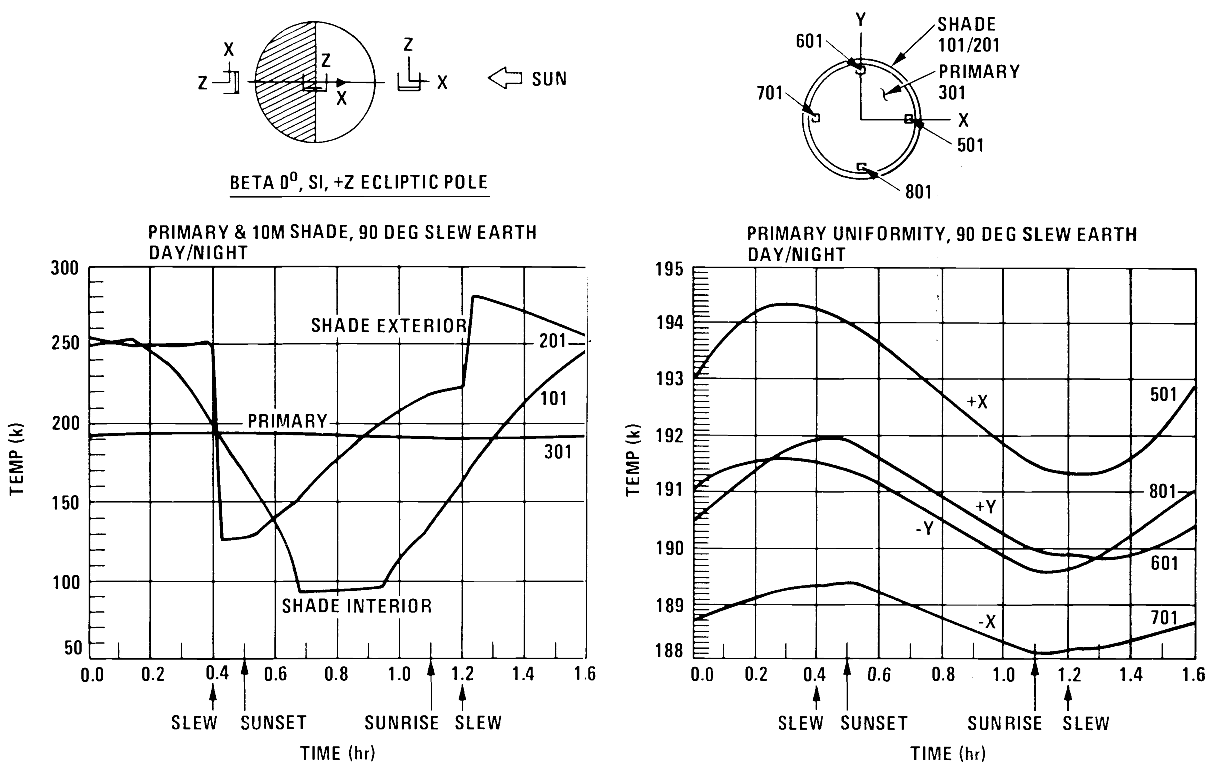

Fig. 11. Thermal performance with 90° slew twice per orbit.

12. THERMAL ANALYSIS

The approach to the thermal analysis and the thermal design concept was to meet the requirements with minimum complexity of the thermal control subsystem. This means using passive thermal control techniques as much as possible. To achieve a passive thermal control subsystem, constraints were placed on the operation of the telescope.

The analysis assumed no direct solar energy on the primary reflector or the interior of its sunshade. Furthermore, the orbital attitude was limited so as to minimize the effects of earth albedo and emission on the primary reflector. The primary reflector was analyzed with a sunshade of various lengths and with an optional aperture lid. The effect of a spacecraft slew was also analyzed to minimize the earth albedo and emission effects.

The selected thermal concept used multilayer insulation and thermal control surfaces as its primary thermal control components. The MLI is used on the sunshade and reflector enclosure. Thermal control techniques, such as aluminized films and black and white paints, are used to control the energy balance for the primary optical system.

The analysis was conducted using the SINDA and LOHARP thermal analyzer tools and was done with appropriate inputs so that temperature predictions were made for dynamic orbital conditions. The thermal system math model consisted of the primary and secondary reflectors, the sunshade, the multilayer insulation around the primary reflector, and the optional aperture lid. There were also four discrete detailed panel math models included in the thermal system model to determine primary reflector temperature gradients, both tangential and normal to the reflector. This model included the external orbital inputs, which consisted of direct solar radiation, earth albedo and emission, and the space sink. This math model was used to develop the preliminary optical system temperature distribution and orbital variation, as shown in Fig. 11.

Table III shows the configurations analyzed, along with the numerical results. Figure 11 shows the dynamic thermal behavior over an orbit for case number 4 (row 4 in Table III). Case number 4 with two large angle slews per orbit and a 10 m sunshade is the most likely configuration.

The analysis shows that the primary reflector can be held below 200 K with a ±2 K uniformity either with spacecraft slewing or with the addition of an aperture lid. The minimum secondary reflector temperature range that can be attained using passive thermal control techniques is 150 K to 175 K.

The primary reflector sunshade can possibly be eliminated if the thermal requirements are relaxed. The primary reflector can be held at 200 K with a uniformity of ±4 K if the spacecraft is slewed twice per orbit, if the sun is not allowed to illuminate the primary reflector or the interior of the sunshade, and if the primary reflector's view of the earth's limb is >25°.

13. CONTROLS AND POINTING

The control subsystem incorporates both the control functions of the attitude and pointing control and the quaternary mirror figure control. The basic attitude information is obtained from the coarse star trackers and the inertial reference unit. The information from the coarse star tracker will be handed over to the fine star tracker, which, during the fine track mode, tracks a guide star that is offset from the astronomical object being observed. A laser beam direction equivalent to the guide star direction is developed and transferred to the fine pointing sensor in the LDR focal plane. The desired relative coordinates of the target image and the guide star

TABLE III. LDR temperature summary (Kelvin).

		Primary reflector				Secondary reflector		
		Orbital		Maximum gradient	Maximum gradient	Orbital		Maximum gradient
Condition	Orientation	Avg.	Swing	edge-edge	front-back	Avg.	Swing	front-back
No slew								
10 m sunshade	+Z eclip pole	196	2.1	4.2	0.04	179	5.0	0.12
10 m sunshade	+Z antisum	237	7.2	1.8	0.07	199	43.9	1.6
10 m sunshade	+Z eclip pole with aperture cover	195	1.6	0.3	0.02	175	2.2	0.05
Slew								
10 m sunshade	Slew 90° twice/orbit	191	2.4	5.1	0.04	162	15.5	0.33
1 m sunshade	Slew 90° twice/orbit	188	3.3	7.0	0.06	173	16.7	0.44

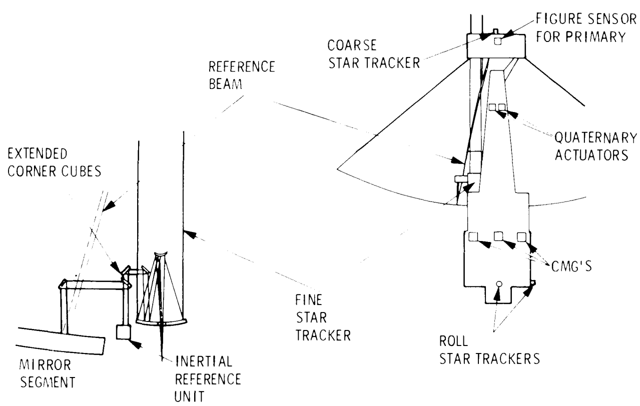

Fig. 12. LDR coarse and fine guidance systems.

image (represented by the laser) on the quadrant detector of the fine pointing sensor are then established. This information is used for coarse and fine control of the line of sight, which are performed by the control moment gyroscopes and the tip and tilt of the overall quaternary mirror, respectively. The optical layout of the coarse and fine guidance system is shown in Fig. 12.

To adjust to an overall rms figure accuracy of 2 μm, the LDR is first pointed to a selected bright object, and its gross figure errors are reduced by the translations and rotations of the whole quaternary mirror using information from the wavefront sensor in the focal plane. In this manner, its figure is acquired and calibrated, and the LDR is then pointed to the target. The figure sensor takes measurements on multiple locations across the primary mirror, providing primary mirror surface errors for figure control. However, the control is not performed at the primary mirror but at quaternary mirror (exit pupil), which is an image of the primary at a 20 to 1 reduced size. Since the figure contol is performed at the quaternary mirror, the figure sensor, measuring only distortions of the primary, would find the same figure errors even if they were already compensated by the quaternary mirror control. Therefore, under this scheme, the quaternary mirror control must remember its previous control positions as the primary mirror distortion changes with respect to time. It is recognized that over a certain amount of time the quaternary mirror control will lose its effectiveness owing to accumulation of sensor and actuator uncertainties. But this problem may be solved either by repeating the figure acquisition and calibration procedure or by installing a second figure sensor to monitor the figure of the quaternary mirror. The combined information from both figure sensors will ensure the effectiveness of the figure control at the quaternary mirror.

14. CONCLUSIONS

By modifying the LDR requirements to exclude the light-bucket mode of operation at wavelengths shorter than 10 μm, by increasing the sun avoidance angle from 60° to 90°, and by spatially chopping at the quaternary rather than the secondary mirror, an LDR concept has been developed that reduces the cost and weight by approximately a factor of 3 over other contemporary concepts. This low-cost, lightweight LDR incorporates two unique design features: (1) lightweight composite reflector panels and (2) two-stage optics. All of the primary science requirements are met at a wavelength of 30 μm.

15. ACKNOWLEDGMENTS

The research described in this paper was carried out by the Jet Propulsion Laboratory, California Institute of Technology, and funded by the Director's Discretionary Fund, under a contract with the National Aeronautics and Space Administration. The study team also included Marjorie P. Meinel, John M. Hedgepeth, Richard Helms, Yu-Hwan Lin, Neville Marzwell, Robert N. Miyake, John E. Stacy, Eldred Tubbs, and Peter G. Wannier. Their contributions are greatly appreciated.

16. REFERENCES

1. G. Field et al., *Astronomy and Astrophysics for the 1980s*, Vol. 1: *Report of the Astronomy Survey Committee*, ISBN 0-309-03249-0, National Academy Press, Washington, D.C. (1982).
2. P. N. Swanson, S. Gulkis, T. B. H. Kuiper, and M. Kiya, "Large Deployable Reflector (LDR): a concept for an orbiting submillimeter-infrared telescope for the 1990s," Opt. Eng. 22(6), 725 (1983).
3. J. B. Breckinridge, P. N. Swanson, A. B. Meinel, and M. P. Meinel, "Perception for a large deployable reflector telescope," in *Advanced Technology Optical Telescopes II*, L. D. Barr and B. Mack, eds., Proc. SPIE 444, 48–52 (1984).
4. P. N. Swanson, J. B. Breckinridge, S. Gulkis, T. B. H. Kuiper, and M. Kiya, "Plans for a large deployable reflector for submillimeter and infrared astronomy from space," in *International Conference on*

Advanced Technology Optical Telescopes, G. Burbidge and L. D. Barr, eds., Proc. SPIE 332, 151–155 (1982).
5. P. N. Swanson and M. Kiya, *Proc. Workshop on Scientific Importance of Submillimeter Observations*, ESA SP-189, European Space Agency, The Netherlands (1982).
6. P. N. Swanson and M. Kiya, "LDR: an orbiting submillimeter-infrared telescope for the 1990s," in *Adaptive Optics Systems and Technology*, R. J. Becherer and B. A. Horwitz, eds., Proc. SPIE 365, 19–30 (1983).
7. D. Hollenbach, ed., *Large Deployable Reflector Science and Technology Workshop*, NASA Conference Publication 2275, Vol. II (1982).
8. P. N. Swanson, "A lightweight low cost Large Deployable Reflector (LDR)," JPL Document D-2283 (1985).
9. S. Von Hoerner, "Surface error and telescope performance for the Large Deployable Reflector," National Radio Astronomy Observatory Engineering Report No. 119 (Dec. 1984).
10. T. B. Vu, Proc. IEEE 116(2), 195–202 (1969).
11. J. E. Stacy, A. B. Meinel, and M. P. Meinel, "Upgrading telescopes by active pupil wavefront correction," in *1985 International Lens Design Conference* (Cherry Hill, N.J., June 10–13, 1985), W. H. Taylor and D. T. Moore, eds., sponsored by OSA and SPIE, Proc. SPIE 554, 186–190 (1986).

Paul N. Swanson was born in San Mateo, Calif., in 1936. After serving in the U.S. Navy, he received his B.S. in physics from the California State Polytechnic University in 1962. He received a Ph.D. degree in physics from The Pennsylvania State University in 1968 and served as a research associate at the Penn State Radio Astronomy Observatory until 1970. Dr. Swanson accepted a full-time faculty position in the Department of Astronomy at Penn State in 1970.

In 1975 Dr. Swanson joined the Jet Propulsion Laboratory, where he managed several microwave projects including the ASSESS II Microwave Limb Sounder Experiment, Millimeter Wavelength Spectroscopy of Interstellar Clouds and Comets from the Kuiper Airborne Observatory, and the Airborne Surveillance Sensor Evaluation Testbed for the U.S. Army. He was surpervisor of the Microwave Atmospheric Sounder Group from 1976 to 1982 and is presently the section manager for Microwave Observational Systems at JPL and manager of the Large Deployable Reflector (LDR) development. He is a member of the AIAA, Sigma XI, AAS, and AAAS.

James B. Breckinridge, Alan Diner, Robert E. Freeland, William R. Irace, Paul M. McElroy, Aden B. Meinel, and **A. Fernando Tolivar:** Biographies and photographs not available.